

Thin film growth models with long surface diffusion lengths

Tung B. T. To, Vitor B. de Sousa, Fábio D. A. Aarão Reis

*Instituto de Física, Universidade Federal Fluminense, Avenida Litorânea s/n, 24210-340
Niterói, RJ, Brazil*

Abstract

In limited mobility (LM) models of thin film deposition, the final position of each atom or molecule is chosen according to a set of stochastic rules before the incidence of another atom or molecule. Here we investigate the possibility of a LM model to reproduce features of a more realistic approach that represents the interplay of collective adatom diffusion and the external flux. In the LM model introduced here, each adatom may execute G hops to neighboring columns of the deposit, but a hop attempt from a site with n lateral neighbors has probability P^n , with $P < 1$. These rules resemble those of the Clarke-Vvedensky (CV) model without energy barriers at step edges, whose main parameters are the diffusion-to-deposition ratio R on terraces and the detachment probability ϵ per lateral neighbor. At short times, the roughness of the LM model can be written in terms of a scaling function of G and P and the growth exponent is consistent with the Villain-Lai-Das Sarma universality class. The evolution of the surface roughness and of the autocorrelation function of the CV model is reproduced with reasonable accuracy by the LM model with suitable choices of parameters. The increase of the parameters G and R of those models produces smoother film surfaces, while the increase of P and ϵ smoothen the terrace boundaries at short lengthscales. However, the detachment probabilities of the two models have very different effects on the surface roughness: in the LM model, for fixed G , the surface roughness increases as P increases; in the CV model, the surface smoothen as ϵ increases, for fixed R . This result is related to the non-Markovian nature of the

Email addresses: tungto@if.uff.br (Tung B. T. To), vitorbds@hotmail.com (Vitor B. de Sousa), reis@if.uff.br (Fábio D. A. Aarão Reis)

LM model, since the diffusivity of an adatom depends on its history at the film surface and may be severely reduced after a detachment from a terrace step; instead, in a collective diffusion model, the detached adatom has the same mobility as a freshly deposited adatom in the same environment. This interpretation is supported by the correlation between the surface roughness and the average number of hops after the last detachment from lateral neighbors in the LM model. We conclude that, although a limited mobility model can reproduce morphological properties of a collective diffusion model, the role of apparently equivalent parameters may be very different, which have consequences for their physical interpretation.

Keywords: thin films, growth models, surface diffusion, dynamic scaling

1. Introduction

Thin film growth models have been intensively studied in the last three decades due to a large number of applications and due to their fundamental interest in non-equilibrium statistical mechanics [1, 2, 3, 4]. The most realistic models describe thermally activated microscopic processes such as diffusion, aggregation, desorption, and chemical reactions which simultaneously occur on the surface of the growing film; energy barriers for diffusion across step edges and various ranges of interactions between adatoms may be considered. The comparison between the parameters used in simulations of these models and those predicted by *ab initio* methods (e. g. density functional theory) may improve the description of a growth process and help the design of films with the desired properties [5]. Among the lattice models of thin film growth [5], one of the simplest examples is the Clarke-Vvedensky (CV) model [6], in which the diffusion coefficients have Arrhenius forms and the energy barriers represent interactions with the nearest neighbors in the lattice. Extensions of the original CV model have applications to molecular beam epitaxy of metals or semiconductors [1, 2, 3, 4, 5, 7], vapor deposition of organic molecules, and deposition of colloidal particles [8, 9, 10, 11].

Thin film growth may also be described with reasonable approximation by limited mobility models, in which the final aggregation position of each deposited atom or molecule is chosen according to a set of stochastic rules before the adsorption of another atom or molecule. Some well-known examples are ballistic deposition [12], the restricted solid-on-solid model [13], and the models for molecular beam epitaxy of Das Sarma and Tamborenea (DT)

[14] and of Wolf and Villain (WV) [15]. Due to their simple growth rules, they are suitable for kinetic roughening studies, which require simulation of large systems and long times. Those studies provide estimates of quantities such as scaling exponents, height, and roughness distributions, which allow the connection between the lattice models and hydrodynamic growth equations that define universality classes [1, 2]. However, an important question is whether limited mobility models with rules that mimic surface diffusion can be related to more realistic approaches such as the CV model.

A limited mobility model with this feature was studied in Ref. [16] and was subsequently termed lateral aggregation of diffusing particles (LADP) [17]. In that model, the incident atom can execute a maximal number of G of hops on terraces and permanently aggregates if it has one or more lateral neighbors. For a suitable choice of parameters, its roughness scaling is the same as that of the CV model with irreversible attachment of adatoms to lateral neighbors; this is a case in which the CV dynamics do not obey detailed balance conditions. The DT, WV, and large curvature models with long diffusion lengths were also studied in several previous works [18, 19, 20, 21], but no relation with models of collective adatom diffusion was proposed. An extension of the LADP model in which atoms with more than one neighbor can move was recently used to describe electrodeposition, in which porous films are formed [22].

In this work, we introduce a limited mobility model which is designed to represent mechanisms of surface diffusion similar to the CV model: each adatom can execute a maximum of G hops, detachment from lateral neighbors is allowed with probabilities depending on its current neighborhood, and solid-on-solid conditions are considered (i. e. the films are not porous). For simplicity, it is hereafter termed LM model. We determine the effects of its parameters on the scaling of the surface roughness and address the question of the equivalence with the original CV model. LM and CV models belong to the universality class of the nonlinear molecular beam epitaxy equation of Villain, Lai, and Das Sarma (VLDS) [23, 24] and we show that it is possible to matching the surface roughness and the autocorrelation function of the two models by a suitable choice of their parameters. However, significant differences are observed in the effects of the probabilities of adatoms detaching from lateral neighbors, which affect the physical interpretation of the LM model. These differences are discussed, with particular emphasis on the effective time of surface diffusion.

The rest of this paper is organized as follows. In Sec. 2, we present

the models, the related growth equation, and the main quantities to be measured. In Sec. 3, we analyze the surface roughness in the LM model. In Sec. 4, we compare results of the LM model with those of the CV model. In Sec. 5, the effects of the detachment from lateral neighbors in the LM model are analyzed. In Sec. 6, we present our conclusions.

2. Basic concepts and definitions

2.1. Models

All models studied here are defined in a simple cubic lattice, with an initially flat substrate at $z = 0$. The edge of a site is taken as the length unit. The lateral size of the lattice is denoted as L and periodic boundary conditions are considered in the x and y directions. The set of adatoms with the same (x, y) position is a column of the deposit; the height variable $h(x, y)$ is the maximal height of an adatom in that column (or the number of atoms in the column).

2.1.1. CV model

Deposition occurs with a flux of F atoms per column per unit time, in the z direction towards the substrate. An incident atom is adsorbed at the top of a randomly chosen column. All adatoms at the top of the L^2 columns are mobile. The hopping rate of an adatom with no lateral neighbor is

$$D_0 = \nu \exp(-E_s/k_B T) \quad (1)$$

where ν is a frequency, E_s is an activation energy, and T is the temperature. If an adatom has n lateral neighbors, its hopping rate is

$$D = D_0 \epsilon^n \quad , \quad \epsilon \equiv \exp(-E_b/k_B T), \quad (2)$$

where E_b is a bond energy. Thus, ϵ may be interpreted as a detachment probability per lateral neighbor. The hop direction is randomly chosen among the four nearest neighbor (NN) columns $(\pm x, \pm y)$ and the adatom moves to the top of that column. Fig. 1 illustrates the possible hops of three adatoms.

In the original CV model, $\nu = 2k_B T/h$, where h is the Planck's constant, as predicted by transition state theory [6]. However, it is more frequent that a constant value $\nu \sim 10^{12} \text{s}^{-1}$ is used in simulation and analytical works [5], and this is also assumed here. The values of E_s and E_b are determined by material properties, while T and F are controlled by the deposition technique.

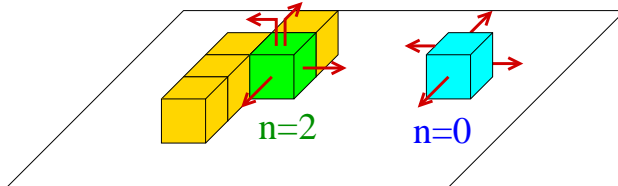


Figure 1: Possible hop directions (red arrows) of adatoms with $n = 0$ (blue), $n = 1$ (brown), and $n = 2$ (green) lateral neighbors; other adatoms are indicated in yellow color.

A diffusion-to-deposition ratio is defined as

$$R \equiv \frac{D_0}{F} = \frac{\nu}{F} \exp(-E_s/k_B T). \quad (3)$$

This is usually interpreted as the number of hops of an adatom in a terrace before it is buried by the next atomic layer. In this work, we consider R and ϵ as the independent parameters of the CV model.

Our simulations are performed in substrates with lateral size $L = 1024$. The simulation time t is expressed as the number of deposited monolayers, which corresponds to $F = 1$. The deposition is limited to 6×10^3 monolayers, which is a typical value for thin films with thicknesses $1\text{-}3\mu\text{m}$. The lattice size is sufficiently large to avoid finite-size effects. We consider the ranges of parameters $10 \leq R \leq 10^4$ and $0 \leq \epsilon \leq 0.1$; this is justified because larger values of R produce films with almost flat surfaces and large values of ϵ represent solids close to the melting points. Average quantities are obtained from 100 independent realizations for each set of parameters.

2.1.2. LM model

In this model, the surface diffusion of each adatom is executed before the next atom is deposited. The adsorption of an incident atom occurs at the top of a randomly chosen column. The diffusion consists of a sequence of G hops to the top of randomly chosen NN columns. Each hop is executed with probability

$$P_{hop} = P^n, \quad (4)$$

where n is the number of lateral neighbors; with probability $1 - P_{hop}$, the hop attempt is rejected. Thus, P is a probability of detachment per lateral neighbor.

The illustration of hop directions in Fig. 1 is also applicable here, although only one adatom is mobile at each time in the LM model. Moreover, the detachment probability proposed in Eq. (4) has the same form as that of the CV model [Eq. (2)]. The LM model is consequently designed with long diffusion lengths and detachment rates that resemble the dynamics of the CV model.

A closer connection might be possible if we assumed that P has an activated form as $P \equiv \exp(-E_P/k_B T)$, where E_P is a bond energy. However, in Sec. 3 we will show that P and ϵ have different effects on the surface roughness, which prevents the interpretation of P as a temperature-like parameter.

The LADP model is the case $P = 0$ [16]. It was already used in studies of apparent anomalies of VLDS models [17] and to simulate effects of surface diffusion in grain coarsening [25]. The electrodeposition model of Ref. [22] is also similar to the LM, but it considers a diffusive flux of incident atoms and the adatom hops allow formation of surface overhangs and, consequently, of porous deposits. The LM model defined here ($P > 0$) was not studied in previous works.

The simulations of the LM model are performed in substrates with lateral size $L = 1024$ and the ranges of parameters $10 \leq G \leq 200$ and $0 \leq P \leq 0.1$. 6×10^3 monolayers are deposited for each set of parameters and average quantities are obtained from 100 realizations. The time unit is also that of deposition of one monolayer.

2.2. Roughness, correlations, and dynamic scaling

The surface roughness is defined as

$$W(L, t) \equiv \left[\left\langle \overline{\langle (h - \bar{h})^2 \rangle} \right\rangle \right]^{1/2}, \quad (5)$$

where the overbars indicate spatial averages and the angular brackets indicate configurational averages. In a kinetic roughening process at relatively short times, the effects of the finite size of the substrate are negligible and the roughness increases as

$$W \sim t^\beta, \quad (6)$$

where β is called the growth exponent. This is termed the growth regime. In the times simulated in this work, the CV and the LM model are in their growth regimes.

The autocorrelation function is defined as [26]

$$\Gamma(s, t) \equiv \frac{\left\langle \left[\tilde{h}(\vec{r}_0 + \vec{s}, t) \tilde{h}(\vec{r}_0, t) \right]^2 \right\rangle}{W^2}, \quad s \equiv |\vec{s}|, \quad (7)$$

where $\tilde{h} \equiv h - \bar{h}$. The configurational averages are taken over different initial positions \vec{r}_0 , different orientations of \vec{s} (substrate directions), and different deposits. This definition implies $\Gamma(0, t) = 1$ and it is generally expected that $\Gamma < 1$ for $s > 0$.

The correlation length ξ may be defined from the correlation function features in different ways. In Ref. [26], the length ξ_e is the first value of s in which $\Gamma(s, t) = e^{-1} \approx 0.3679$. A correlation length ξ_0 may be defined as the first zero of the correlation function, $\Gamma(\xi_0, t) = 0$; this may be particularly useful to characterize surfaces with mounded structure. In all cases, ξ is a typical length with significant height fluctuations. In the growth regime, it is expected that $\xi \sim t^z$, where z is the dynamical exponent.

When growth is dominated by surface diffusion, it is expected to be described by a fourth order stochastic equation in the hydrodynamic limit [1]:

$$\frac{\partial h(\vec{r}, t)}{\partial t} = \nu_4 \nabla^4 h + \lambda_4 \nabla^2 (\nabla h)^2 + \eta(\vec{r}, t), \quad (8)$$

where $h(\vec{r}, t)$ is the height at position \vec{r} and time t in a d -dimensional substrate, ν_4 and λ_4 are constants and η is a Gaussian, nonconservative noise [the contribution of the average external flux is omitted in Eq. (8)]. The linear version ($\lambda_4 = 0$) is the Mullins-Herring (MH) equation [27] and the nonlinear version ($\lambda_4 \neq 0$) is the VLDS equation [23, 24]. In $2 + 1$ dimensions, the best numerical estimates of scaling exponents of the VLDS class are $\beta \approx 0.20$ and $z \approx 3.3$ [28, 29, 30, 31]. They agree with the two-loop renormalization estimates $\beta \approx 0.199$ and $z \approx 3.36$ [32].

The CV model is described by the VLDS equation in the continuous limit, as shown by renormalization studies [33, 34] and by numerical calculation of scaling exponents (growth, dynamical, and the roughness exponent $\alpha = \beta z$) [35, 36, 37, 38]. For the values $\epsilon \leq 0.1$ studied here and with no energy barrier at terrace steps, no crossover or instability is expected in the CV model at long times; for $\epsilon \sim 0.25$ or larger, the system without deposition is close to a roughening transition, and instabilities appear when step barriers are included, but these phenomena will not be addressed here. The exponents of

the LADP model ($P = 0$) were also shown to be consistent with the VLDS class [16].

3. Surface roughness in the LM model

Figs. 2(a)-(d) show top views of films deposited with two values of G and two values of P . These images have lateral size 100, which is much smaller than the total size of the deposits, but is suitable for visualization of small lengthscale features.

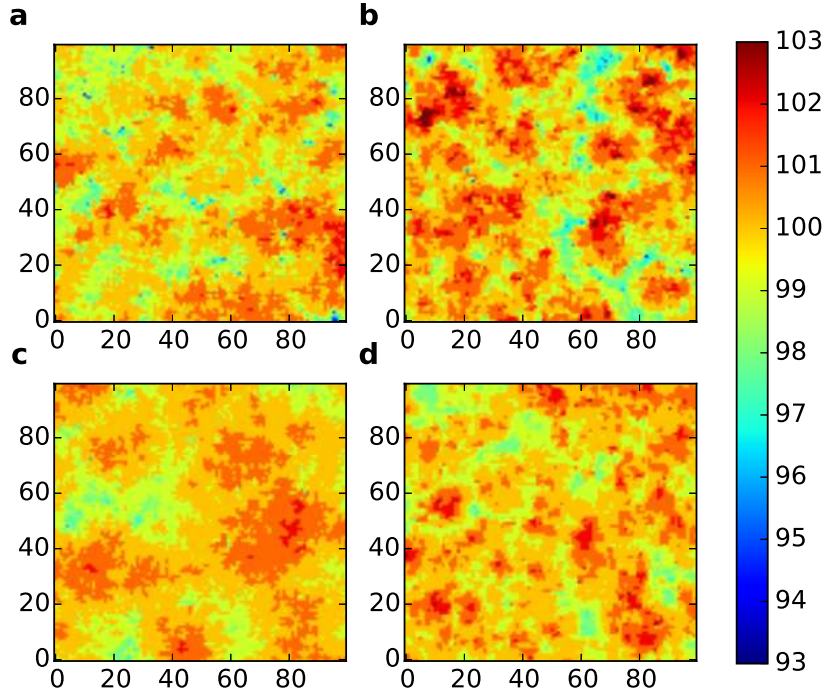


Figure 2: Top views of films deposited with the LM model at $t = 100$ with parameters (a) $G = 20$, $P = 0$; (b) $G = 20$, $P = 0.1$; (c) $G = 60$, $P = 0$; (d) $G = 60$, $P = 0.1$.

For $P = 0$, the terraces have highly disordered boundaries which resemble diffusion-limited aggregates [39]; this morphology is observed since the early stages of deposition, when a submonolayer is being formed [5]. The average terrace size clearly increases with G .

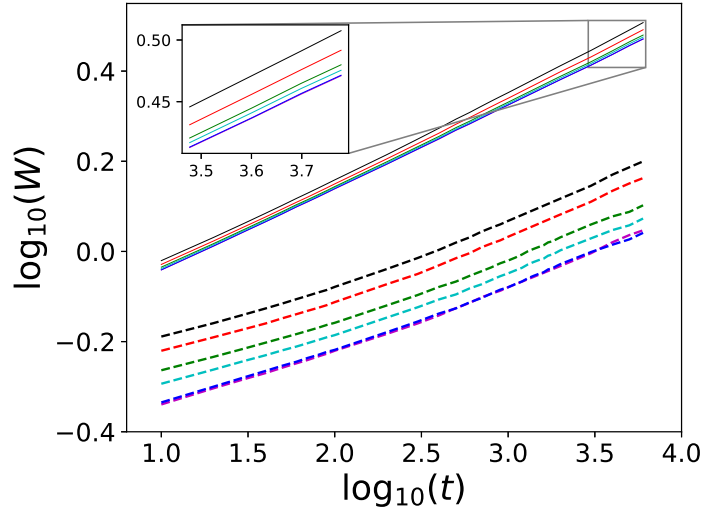


Figure 3: Roughness as a function of time of the LM model with $G = 10$ (solid lines) and $G = 100$ (dashed lines). From bottom to top, the values of P are 0, 0.001, 0.01, 0.02, 0.05, and 0.1.

For $P > 0$, careful inspection of the images in Figs. 2(b) and 2(d) show terrace boundaries with some straight regions, particularly for $G = 60$. Such effect is expected because the detachment of weakly bonded adatoms at terrace borders permits their diffusion until reaching more stable positions, i. e. positions with larger numbers of lateral neighbors. However, the straight regions seldom have more than 10 adatoms, so the terrace boundaries are highly disordered in longer length scales.

Figs. 3 show the evolution of the surface roughness of the LM model with two values of G and several values of P . For fixed P , the increase in G has a smoothing effect; for $G = 100$, $W \lesssim 1$ at all simulated times, which means that the film surfaces have typical fluctuations smaller than the size of an adatom. This explains why large values of G were not considered here. For fixed G , we observe that the increase in P leads to an increase in the roughness, even for very small values of this parameter. This is a surprising effect because increasing P has a smoothing effect on the terrace borders.

Note that there is no inconsistency in the effects of P on the roughness and on the terrace boundaries. The main contribution to the roughness is given by the long wavelength fluctuations in the vertical (z) direction,

while fluctuations in terrace borders are measured in small lengthscales in the directions parallel to the substrate (x and y).

The dynamic scaling relation (Family-Vicsek relation [40]) can incorporate the non-universal parameters G and P . The dependence of the roughness on G is predicted by a scaling approach [16, 37] and the incorporation in the scaling relation follows the same lines of works on competitive growth models [41, 42]. However, there is no such approach to predict the dependence on ϵ , thus our procedure is to search for the simplest possible relation that fits the numerical data; this procedure was adopted in the study of the CV model in Ref [37].

First, we expect that the roughness scales as $W \sim t^{0.2}/G^{0.5}$ for $P = 0$, as shown by scaling arguments in Ref. [16]. This means that the scaled time variable need to have the form $t/G^{5/2}$. Second, the plots of the roughness for fixed G in Fig. 3 suggest an approximately linear increase of the roughness with P , for fixed time. This leads to the proposal

$$W \approx f \left[\frac{t}{G^{5/2}} (G^\delta P + b)^\gamma \right], \quad (9)$$

where f is a scaling function and δ , γ , and b are constants. The apparent linearity of the roughness with P suggests that $\gamma \approx 1$, but we do not have any theoretical explanation to this result. We also do not have any argument to anticipate the values of δ and b .

Fig. 4 shows W as a function of the scaling variable of Eq. (9), for $\delta = 1.3$, $\gamma = 0.9$, and $b = 2.5$; these are the values which provide the best collapse of the data into a single curve. The slope at the longest times is very close to 0.20, which agrees with the VLDS class. The proposed scaling form also confirms the general trend of W to increase with G (for fixed P) and to increase with P (for fixed G).

4. Comparison between LM and CV models

Since the LM and the CV models have VLDS scaling [Eq. (6)] with small corrections at short times, we expect that for some sets of parameters they show the same evolution of the surface roughness. For $\epsilon = P = 0$, this occurs if $G \approx 0.29R^{0.6}$ [16]. Figs. 5(a)-(b) show the matching of the roughness evolution for $\epsilon = P > 0$ with a suitable choice of G for each values of R . This matching is also possible for $\epsilon \neq P$ with suitable choices of R and G .

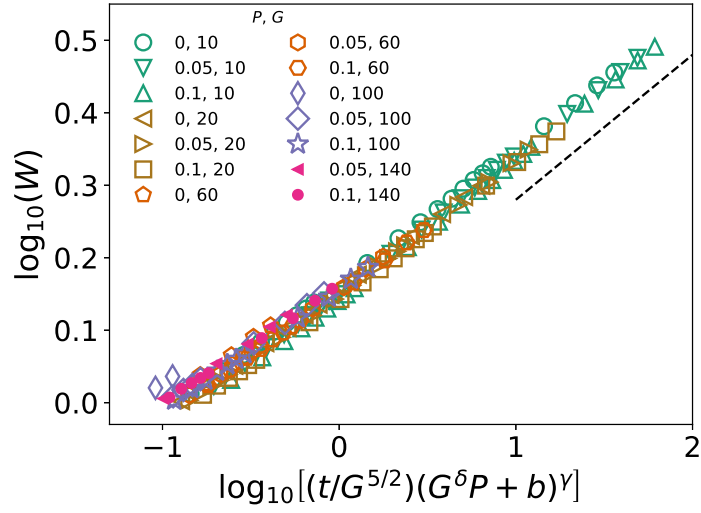


Figure 4: Roughness as a function of the time scaled according to Eq. (9), with $\delta = 1.3$, $\gamma \approx 0.9$, and $b = 2.5$. The dashed line has slope 0.20.

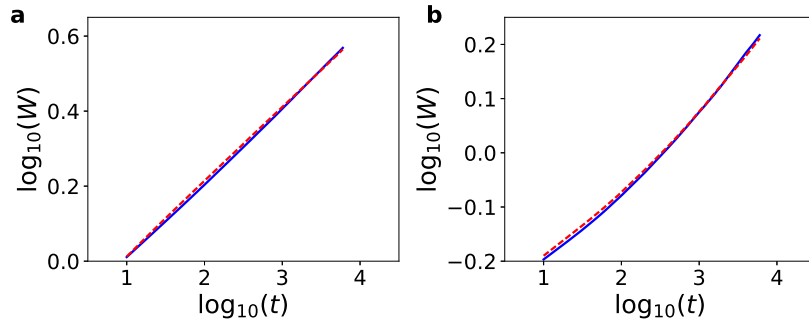


Figure 5: Comparison of the roughness evolution of the LM and CV models, with: (a) $R = 10^2$, $\epsilon = 0.05$ (solid line), $G = 7$, $P = 0.05$ (dashed line); (b) $R = 10^3$, $\epsilon = 0.1$ (solid line), $G = 89$, $P = 0.1$ (dashed line).

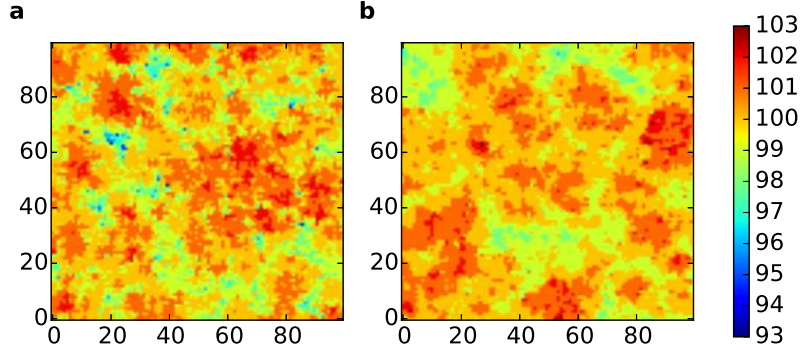


Figure 6: Top views of the surfaces grown with the CV model with: (a) $R = 10^2$, $\epsilon = 0.05$ and (b) $R = 10^3$, $\epsilon = 0.1$.

Figs. 6(a)-(b) show top views of the film surfaces grown with the CV model with the same parameters of Figs. 5(a)-(b). The average terrace size increases with R , which parallels the increase with G in the LM model [Figs. 2(a)-(d)]. Terrace boundaries are also very rough. For constant R , the increase of ϵ leads to the formation of a larger number of straight regions in the terrace borders. Indeed, the detachment of an adatom from a position with small number of lateral neighbors permits that it moves until reaching a point with higher coordination, where it remains for a long time and may be eventually covered by a new atomic layer. Thus, the effects of P and ϵ on terrace boundaries are also similar. However, increasing the detachment probability ϵ has a smoothening effect [37], which contrasts with the roughening effect of P .

The comparison of the correlation functions of the surfaces with the same roughness grown by the two models confirm that those surfaces are similar. Figs. 7(a)-(b) show $\Gamma(s, t = 6000)$ as a function of the distance s , for the same model parameters of Figs. 5(a)-(b). For small s , the curves of the two models usually collapse, which means that the estimates of the correlation length ξ are approximately the same. There may be difference of a few percents near the first minimum, as shown in Fig. 5(a), which leads to

small differences in the correlation length ξ_0 . There are other parameter sets $[(G, P)$ and $(R, \epsilon)]$ which produce the same roughness evolution and autocorrelation functions with small differences.

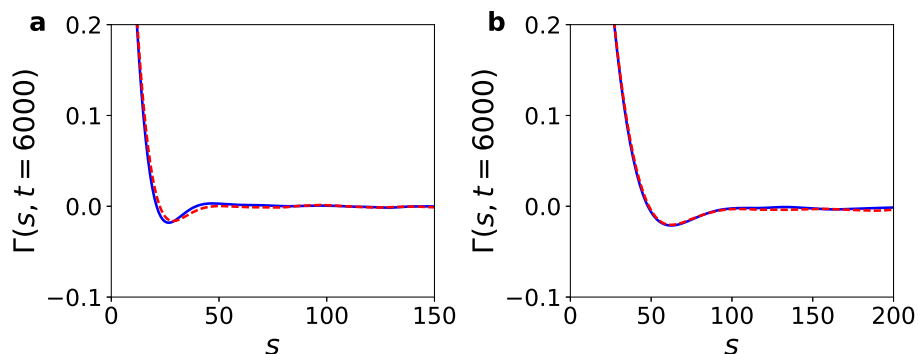


Figure 7: Comparison of the correlation function of the LM and CV models at $t = 6000$ for the same parameters as in Fig. 5(a)-(b).

In Ref. [37], a scaling relation analogous to Eq. (9) was obtained for the CV model in the growth regime:

$$W \sim \left[\frac{t}{R^{3/2}(\epsilon + a)} \right]^{0.2}, \quad (10)$$

where $a = 0.025$ is a fit parameter. This relation is consistent with VLDS scaling. The combination of this result and Eq. (9) imply that the same roughness scaling at short times is obtained in the CV and LM models under the condition

$$R \sim \frac{G^{5/3}}{(\epsilon + a)^{2/3}(G^\delta P + b)^{2\gamma/3}}. \quad (11)$$

This relation is presented here for completeness, but it does not add any information on the physics of the models because it involves four fit parameters (a , b , δ , and γ). However, since the effect of ϵ is small, it may be helpful to predict the order of magnitude of the parameter R whose results can be approximated by this LM model.

5. The effects of detachment probabilities in the LM model

5.1. Numerical results

The nontrivial effect of the detachment probability P on the roughness is also illustrated by the comparison of surfaces with the same roughness grown by the LM model with different parameters. In Table 1, we show the parameters G and P which give three chosen values of W at $t = 6000$. As P increases from 0 to 0.1, the values of G which provide the same roughness may increase by a factor close to 3.

Table 1: The values of the parameters G and P which provide the given values of the roughness at time $t = 6000$ and the corresponding average number of hops of adatoms since the adsorption and since the last detachment.

$W (t = 6000)$	G	P	$\langle N \rangle$	$\langle N_{last} \rangle$
2.30	16	0	1.979(1)	1.979(1)
	20	0.05	2.6925(5)	1.8865(5)
	24	0.1	3.672(1)	1.7225(5)
1.73	29	0	3.333(1)	3.333(1)
	48	0.05	5.866(1)	3.147(1)
	68	0.1	9.595(2)	2.659(1)
1.63	33	0	3.727(2)	3.727(2)
	60	0.05	7.138(2)	3.497(1)
	89	0.1	12.228(2)	2.874(1)

We measured the average number of hops executed by an adatom, $\langle N \rangle$, for each parameter set. This may be interpreted as the average diffusion time of the adatom since its adsorption, but excluding the time attached to lateral neighbors. The values of $\langle N \rangle$ are shown in Table 1. They clearly have remarkable differences for the films with the same roughness.

Fig. 8 shows $\langle N \rangle$ as a function of G for three values of P . It shows that $\langle N \rangle$ linearly increases with G , with weaker dependence on P . As G increases by 10 units, $\langle N \rangle$ typically increases by 1.1-1.3 units.

We also calculated the average number of hops executed by the adatoms after the last detachment from a terrace border, $\langle N_{last} \rangle$. If there is no detachment during the adatom diffusion, then the total number of hops is considered in this average. The values of $\langle N_{last} \rangle$ are shown in Table 1 and plotted in Fig. 8. The data for $P > 0$ is clearly below the red fitting line for $P = 0$, which means that the increase of P leads to a significant decrease of $\langle N_{last} \rangle$,

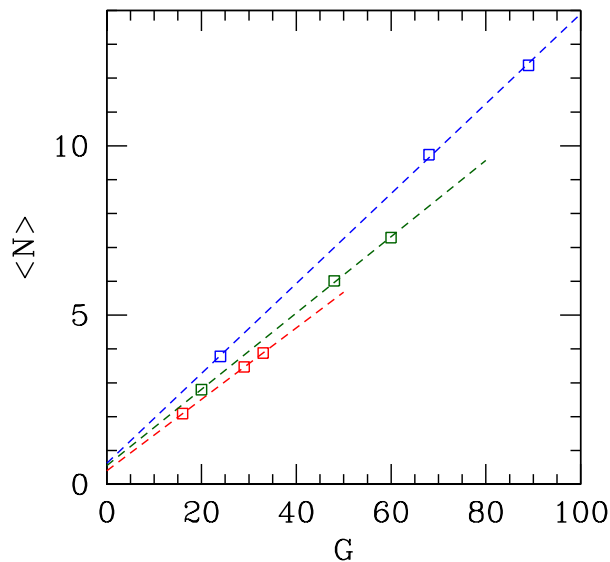


Figure 8: Average numbers of hops (total and after the last detachment) as a function of G for three values of P . The dashed lines are least squares fits of $\langle N \rangle$ for each P , with slopes 0.103, 0.112, and 0.132 from bottom to top.

for fixed G . This contrasts with the increase of $\langle N \rangle$ with P and means that detachment events are frequent for $P > 0$.

5.2. Interpretation of the results

When an adatom detaches from a lateral neighbor, it frequently moves to a terrace, at the same level or at an upper level; see Fig. 1. After the detachment, there is a significant difference in the adatom mobility in the LM and in the CV model. In the CV model, this adatom has the same diffusion coefficient of all other terrace adatoms with the same neighborhood, independently of the time in which they were deposited. However, in the LM model, the detached adatom will execute less than G hops; consequently, it has a smaller mobility than a freshly deposited atom. In simple words, the detached adatom in LM is a "tired adatom".

In many cases, after the detachment from a terrace border, the adatom moves to the site where it came from before the attachment, i. e. it begins moving from the same position where it was before attaching to that bor-

der. In the LM model, this adatom can execute a smaller number of hops in comparison with the first visit to that position; this is consistent with the decrease of $\langle N_{last} \rangle$ with P , as shown in Fig. 8. This helps to explain why $(G, P > 0)$ may produce the same morphology which is produced by $(G', P = 0)$ with $G' < G$, i. e. with a smaller number of available hops and irreversible lateral aggregation.

In Fig. 8, it is also noticeable that the values of $\langle N_{last} \rangle$ are not very different for the model parameters that produce the same roughness. This indicates that the diffusion time after the last detachment, $\langle N_{last} \rangle$, is correlated with the surface roughness, which tends to decrease as $\langle N_{last} \rangle$ increases. Instead, the total number of hops of an adatom, $\langle N \rangle$, is not correlated with the roughness. This corroborates the interpretation that, for constant G , the increase of the number of detachment events leads to an increase in the number of "tired adatoms" at the surface, which increases the surface disorder.

The parameter ϵ in the CV model has the opposite effect on the surface roughness. The adatom is not "tired" after the detachment from a terrace step; it has the same dynamics as a freshly deposited atom. The role of ϵ is to hold the adatom in an energetically favorable position for a certain time (typically $\sim \epsilon^{-(n-1)}$), where it may be buried by the next deposited layer (permanent attachment). As ϵ increases, positions with small n become less favorable, so that permanent attachment tends to occur at positions with larger n . This is clearly observed in simulations of submonolayer growth [43]. The preferential attachment at positions with larger n produces more compact structures and explains the decrease of roughness with ϵ , for fixed R .

The nontrivial results for the LM model are related to the non-Markovian rule for adatom diffusion. This feature leads to very different diffusion properties when compared to Markovian models. An example is the non-Markovian random walk studied in Ref. [44] (a generalization of the elephant random walk [45]), in which a hop to a NN site has a probability that decreases in time as a power law with exponent $-\lambda$. In the case of unbiased walks, subdiffusion is observed for $0 < \lambda \leq 1$, but for larger λ the walker is stationary, i. e. its characteristic displacement has a finite asymptotic value. This contrasts with the normal diffusion in the case where a hop has a finite probability to be executed. In our model of adatom diffusion, the condition of a maximal number of G hops corresponds to an infinitely rapid time decay of the hopping probability at $t = G$ (i. e. a decay much faster than any continuous function). Moreover, using a Langevin equation approach, it

was shown in Ref. [46] that a system with exponentially decreasing memory kernel in contact with a reservoir may have anomalous thermalization [46]; note that this is a case with memory of much shorter range than models of the type of the elephant random walk [45].

On the other hand, the Markovian property must not be viewed as a necessary condition for a model to describe adatom diffusion on surfaces. For instance, Ref. [47] showed that a coarse-grained non-Markovian model was necessary to reproduce the motion of adsorbed molecules in microporous materials predicted by molecular dynamics simulations. Here, the non-Markovian LM model was actually able to provide results consistent with the CV model, although the apparently corresponding parameters ϵ and P have different effects on the surface roughness.

6. Conclusion

We introduced a limited mobility model with long surface diffusion lengths of the adsorbed atoms and with reversible aggregation to lateral neighbors during its diffusion (LM). These are the same conditions of the simplest model that describes the simultaneous effects of deposition and collective surface diffusion in thin film growth (CV). We investigated the scaling properties of the LM model, compared them with the CV model, and discussed the effects of the probabilities of detachment from terrace steps.

The maximal number of hops in the LM model, G , plays a similar role as the diffusion-to-deposition ratio R in the CV model, since both parameters are related to the average diffusion time in terraces. Indeed, the roughness has a significant decrease as G or R increases. In short length scales, increasing P or ϵ has the effect of forming longer straight regions in the terrace boundaries. For given R and ϵ in the CV model, it is possible to find pairs (G, P) which lead to the same evolution of the surface roughness and reasonable agreement between the corresponding autocorrelation functions. This shows that a properly defined model with limited mobility can reproduce the surface fluctuations and correlations a more realistic growth model. For this reason, it may be interesting to extend limited mobility models to consider mechanisms such as energy barriers at descending steps or anisotropic diffusion.

However, there is a striking difference between the effects of the detachment probabilities P and ϵ on the surface roughness, since the increase of

P leads to the increase of the roughness. While ϵ can be related to an activation energy and the temperature [Eq. (2)], a similar interpretation for P becomes difficult. The nontrivial effect of P is related to the reduced diffusion time of an adatom in the LM model after it detaches from a step edge, i. e. the number of available hops for this adatom is smaller than the number of hops available for a freshly deposited adatom. On the other hand, in the CV model, all atoms with the same neighborhood have the same diffusion coefficient, independently of their history at the film surface. Quantitatively, we observe that the surface roughness in the LM model is correlated with the average number of hops of an adatom after the last detachment from lateral neighbors, $\langle N_{last} \rangle$. Instead, the average number of hops since the adsorption, $\langle N \rangle$, cannot explain the variations of the roughness.

These results suggest that a limited mobility model with a maximal number of allowed hops will always provide a limited description of a real growth process dominated by surface diffusion. One possibility for future work is to improve the design of the limited mobility models with parameters that may be interpreted in a similar way as those of the collective diffusion models. For instance, the present model may be extended by allowing the adatom at a terrace to execute G hops even after detachment from a terrace step; this adatom still holds a memory on the number of previously executed hops, but the depletion of $\langle N_{last} \rangle$ as P increases may be suppressed.

Acknowledgment

The authors acknowledge support from CNPq, CAPES, and FAPERJ (Brazilian agencies).

References

- [1] A.-L. Barabási and H. E. Stanley. Fractal Concepts in Surface Growth. Cambridge University Press, New York, USA, 1995.
- [2] Joachim Krug. Origins of scale invariance in growth processes. Advances in Physics, 46(2):139–282, 1997.
- [3] A. Pimpinelli and J. Villain. Physics of Crystal Growth. Cambridge University Press, 1998.
- [4] T. Michely and J. Krug. Islands, Mounds, and Atoms. Springer, 2003.

- [5] J.W. Evans, P.A. Thiel, and M.C. Bartelt. Morphological evolution during epitaxial thin film growth: Formation of 2d islands and 3d mounds. Surface Science Reports, 61(1):1 – 128, 2006.
- [6] S. Clarke and D. D. Vvedensky. Growth kinetics and step density in reflection high-energy electron diffraction during molecular-beam epitaxy. J. Appl. Phys., 63:2272, 1988.
- [7] Mario Einax, Wolfgang Dieterich, and Philipp Maass. Colloquium: Cluster growth on surfaces: Densities, size distributions, and morphologies. Rev. Mod. Phys., 85:921–939, Jul 2013.
- [8] R. Ganapathy, M. R. Buckley, S. J. Gerbode, and I. Cohen. Direct measurements of island growth and step-edge barriers in colloidal epitaxy. Science, 327:445–448, 2010.
- [9] Paulette Clancy. Application of molecular simulation techniques to the study of factors affecting the thin-film morphology of small-molecule organic semiconductors. Chemistry of Materials, 23(3):522–543, Feb 2011.
- [10] S. Bommel, N. Kleppmann, C. Weber, H. Spranger, P. Schäfer, J. Novak, S. V. Roth, F. Schreiber, S. H. L. Klapp, and S. Kowarik. Unravelling the multilayer growth of the fullerene C₆₀ in real time. Nat. Commun., 5:5388, 2014.
- [11] N. Kleppmann, F. Schreiber, and S. H. L. Klapp. Limits of size scalability of diffusion and growth: Atoms versus molecules versus colloids. Phys. Rev. E, 95:020801(R), 2017.
- [12] Marjorie J. Vold. Sediment volume and structure in dispersions of anisometric particles. The Journal of Physical Chemistry, 63(10):1608–1612, Oct 1959.
- [13] Jin Min Kim and J. M. Kosterlitz. Growth in a restricted solid-on-solid model. Phys. Rev. Lett., 62:2289–2292, May 1989.
- [14] S. Das Sarma and P. Tamborenea. A new universality class for kinetic growth: One-dimensional molecular-beam epitaxy. Phys. Rev. Lett., 66:325–328, Jan 1991.

- [15] D.E. Wolf and J. Villain. Growth with surface diffusion. EPL (Europhysics Letters), 13(5):389, 1990.
- [16] F. D. A. Aarão Reis. Dynamic scaling in thin-film growth with irreversible step-edge attachment. Phys. Rev. E, 81:041605, Apr 2010.
- [17] F. D. A. Aarão Reis. Normal dynamic scaling in the class of the nonlinear molecular-beam-epitaxy equation. Phys. Rev. E, 88:022128, 2013.
- [18] S. Das Sarma, P. Punyindu Chatraphorn, and Z. Toroczkai. Universality class of discrete solid-on-solid limited mobility nonequilibrium growth models for kinetic surface roughening. Phys. Rev. E, 65:036144, Mar 2002.
- [19] P. Punyindu Chatraphorn and S. Das Sarma. Layer-by-layer epitaxy in limited mobility nonequilibrium models of surface growth. Phys. Rev. E, 66:041601, Oct 2002.
- [20] P. Disrattakit, R. Chanphana, and P. Chatraphorn. Roughness distribution of multiple hit and long surface diffusion length noise reduced discrete growth models. Physica A: Statistical Mechanics and its Applications, 462:619 – 629, 2016.
- [21] P. Disrattakit, R. Chanphana, and P. Chatraphorn. Skewness and kurtosis of height distribution of thin films simulated by larger curvature model with noise reduction techniques. Physica A: Statistical Mechanics and its Applications, 484:299 – 308, 2017.
- [22] F. D. A. Aarão Reis, Dung di Caprio, and Abdelhafed Taleb. Crossover from compact to branched films in electrodeposition with surface diffusion. Phys. Rev. E, 96:022805, Aug 2017.
- [23] J. Villain. Continuum models of crystal growth from atomic beams with and without desorption. J. Phys. I France, 1(1):19–42, 1991.
- [24] Z.-W. Lai and S. Das Sarma. Kinetic growth with surface relaxation: Continuum versus atomistic models. Phys. Rev. Lett., 66:2348–2351, May 1991.
- [25] F. D. A. Aarão Reis. Effects of film growth kinetics on grain coarsening and grain shape. Phys. Rev. E, 95:042805, 2017.

- [26] Y. Zhao, G.-C. Wang, and T.-M. Lu. Characterization of Amorphous and Crystalline Rough Surface: Principles and Applications. Academic Press, San Diego, CA, USA, 2001.
- [27] W. W. Mullins. Theory of thermal grooving. J. Appl. Phys., 28:333–339, 1957.
- [28] F. D. A. Aarão Reis. Numerical study of discrete models in the class of the nonlinear molecular beam epitaxy equation. Phys. Rev. E, 70:031607, Sep 2004.
- [29] Géza Ódor, Bartosz Liedke, and Karl-Heinz Heinig. Surface pattern formation and scaling described by conserved lattice gases. Phys. Rev. E, 81:051114, May 2010.
- [30] H. Xia, G. Tang, Z. Xun, and D. Hao. Numerical evidence for anomalous dynamic scaling in conserved surface growth. Surf. Sci., 607:138–147, 2013.
- [31] I. S. S. Carrasco and T. J. Oliveira. Universality and dependence on initial conditions in the class of the nonlinear molecular beam epitaxy equation. Phys. Rev. E, 94:050801(R), 2016.
- [32] H. K. Janssen. On critical exponents and the renormalization of the coupling constant in growth models with surface diffusion. Phys. Rev. Lett., 78:1082, 1997.
- [33] C. A. Haselwandter and D. D. Vvedensky. Fluctuation regimes of driven epitaxial surfaces. EPL (Europhysics Letters), 77(3):38004, 2007.
- [34] Christoph A. Haselwandter and Dimitri D. Vvedensky. Renormalization of stochastic lattice models: Epitaxial surfaces. Phys. Rev. E, 77:061129, Jun 2008.
- [35] M. Kotrla and P. Smilauer. Nonuniversality in models of epitaxial growth. Phys. Rev. B, 53:13777–13792, 1996.
- [36] F. F. Leal, S. C. Ferreira, and S. O. Ferreira. Modelling of epitaxial film growth with an Ehrlich-Schwoebel barrier dependent on the step height. Journal of Physics: Condensed Matter, 23(29):292201, 2011.

- [37] T. A. de Assis and F. D. A. Aarão Reis. Dynamic scaling and temperature effects in thin film roughening. Journal of Statistical Mechanics: Theory and Experiment, 2015(6):P06023, 2015.
- [38] Edwin E. Mozo Luis, Thiago A. de Assis, and Silvio C. Ferreira. Optimal detrended fluctuation analysis as a tool for the determination of the roughness exponent of the mounded surfaces. Phys. Rev. E, 95:042801, Apr 2017.
- [39] T. A. Witten Jr. and L. M. Sander. Diffusion-limited aggregation, a kinetic critical phenomenon. Phys. Rev. Lett., 47:1400–1403, 1981.
- [40] F. Family and T. Vicsek. Scaling of the active zone in the eden process on percolation networks and the ballistic deposition model. J. Phys. A: Math. Gen., 18:L75, 1986.
- [41] C. M. Horowitz and E. V. Albano. Dynamic properties in a family of competitive growing models. Phys. Rev. E, 73:031111, 2006.
- [42] Y.-L. Chou and M. Pleimling. Parameter-free scaling relation for nonequilibrium growth processes. Phys. Rev. E, 79:051605, 2009.
- [43] T. J. Oliveira and F. D. A. Aarão Reis. Scaling in reversible submonolayer deposition. Phys. Rev. B, 87:235430, Jun 2013.
- [44] M. A. A. da Silva, G. M. Viswanathan, and J. C. Cressoni. Ultraslow diffusion in an exactly solvable non-markovian random walk. Phys. Rev. E, 89:052110, 2014.
- [45] M. A. Schutz and S. Trimper. Elephants can always remember: Exact long-range memory effects in a non-markovian random walk. Phys. Rev. E, 70:045101, 2004.
- [46] L. C. Lapas, R. M. S. Ferreira, J. M. Rub, and F. A. Oliveira. Anomalous law of cooling. J. Chem. Phys., 142:104106, 2015.
- [47] A. M. Pintus, A. Gabrieli, F. G. Pazzona, P. Demontis, and G. B. Sufritti. A coarse-grained method based on the analysis of short molecular dynamics trajectories for the simulation of non-markovian dynamics of molecules adsorbed in microporous materials. J. Chem. Phys., 141:074109, 2014.